Düzce University
Journal of Science & Technology

Research Article

Three-phase Active Tracking AC-AC Voltage Regulator based on Buck Converter with an Efficient Hybrid Control Technique

Faruk YALÇIN [a,*], Felix A. HIMMELSTOSS [b]

[a] *Department of Mechatronics Engineering, Faculty of Technology, Sakarya University of Applied Sciences, Sakarya, TURKEY*
[b] *Department of Electronic Engineering, University of Applied Sciences Technikum Wien, Vienna, AUSTRIA*
** Corresponding author's e-mail address: farukyalcin@sakarya.edu.tr*
DOI: 10.29130/dubited.923829

ABSTRACT

This study proposes a switch-mode three-phase active tracking AC-AC voltage regulator based on the buck converter. The regulator topology incorporates a moderate number of components with less complexity and high efficiency. An efficient hybrid control technique, based on a closed-loop PID controller that is supported with a new designed feedforward controller, is proposed for the regulator control different to the similar studies in the literature. The hybrid control technique augments the response of active tracking of the reference output phase voltages to achieve an improved quality close to sine-wave output phase voltages for either the input AC phase voltages that are ideal pure sine-wave or include various harmonics. The regulator topology has a modular structure for independent control of each output phase. So, the regulator can help to achieve close to sine-wave output phase voltages to supply a balanced/unbalanced wye-connected three-phase load or independent single-phase loads. The presented three-phase regulator and the control technique are tested with simulation and experimental studies. The laboratory set-up of the regulator is designed for 2.2 kW output power, 0-300 Vp input phase voltages (50 Hz), and 0-200 Vp output phase voltages. The results demonstrated that the proposed switch-mode three-phase buck-type active tracking voltage regulator can provide the desired AC phase voltages with less than 5% THD (total harmonic distortion) and low harmonics for different operating conditions.

Keywords: *Buck converter, AC-AC regulator, Three-phase, Active tracking, THD*

Etkili Bir Hibrit Kontrol Tekniği ile Alçaltıcı Çevirici Tabanlı Üç Faz Aktif İzleyen AA-AA Gerilim Regülatörü

ÖZ

Bu çalışma, alçaltıcı çevirici tabanlı anahtarlamalı mod aktif izleyen bir AA-AA gerilim regülatörü sunmaktadır. Regülatör topolojisi az karmaşıklık ve yüksek verimlilik sağlayacak şekilde makul sayıda eleman içermektedir. Literatürdeki benzer çalışmalardan farklı olarak, bu çalışmada regülatörün kontrolü için kapalı çevrim PID kontrolcünün yeni tasarlanan bir ileri beslemeli kontrolcü ile desteklenmesi tabanlı etkili bir hibrit kontrol tekniği önerilmiştir. Hibrit kontrol tekniği, giriş AA faz gerilimlerinin ideal saf sinüs dalgası olması ya da farklı harmonikler içermesi durumunda dahi iyileştirilmiş kalitede sinüs formuna yakın çıkış faz gerilimlerinin elde edilebilmesi için referans çıkış faz gerilimlerinin aktif izlenmesi cevabını arttırmaktadır. Regülatör topolojisi her bir çıkış fazının bağımsız olarak kontrol edilebilmesini sağlayan modüler bir yapıya sahiptir. Böylelikle regülatör, dengeli/dengesiz yıldız bağlı üç fazlı bir yükün ya da birbirinden bağımsız tek fazlı yüklerin beslenmesi için sinüs dalga formuna yakın çıkış faz gerilimlerinin elde edilebilmesine yardımcı olmaktadır. Sunulan üç fazlı regülatör ve kontrol tekniği simülasyon ve deneysel çalışmalarla test edilmiştir. Regülatöre ait laboratuvar test düzeneği 2.2 kW çıkış gücü, 0-300 Vp giriş faz gerilimleri (50 Hz) ve 0-200 Vp çıkış faz

Received: 20/04/2021, Revised: 08/07/2021, Accepted: 29/07/2021

gerilimleri için tasarlanmıştır. Elde edilen sonuçlar, önerilen anahtarlamalı mod üç faz alçaltıcı tip aktif izlemeli gerilim regülatörünün farklı çalışma koşullarında %5 ten az THD (toplam harmonik distorsiyonu) değerine sahip istenen AA faz gerilimlerini sağlayabildiğini göstermektedir.

Anahtar Kelimeler: *Alçaltıcı çevirici, AA-AA regülatörü, Üç faz, Aktif izleyen, THD*

I. INTRODUCTION

One of the major problems of AC loads in power systems is decreasing power quality caused by increasing electrical power demand. AC loads, need to be supplied by alternating voltages with determined acceptable voltage magnitudes, where most of the AC loads require nearly constant magnitudes of the phase voltages. Transient effects in distribution systems decrease the power quality of the AC loads and lead to voltage sags or voltage swells. In addition, variable AC voltages (not the same as the constant grid voltages) may be required for some AC loads in applications such as motor controls. Depending on the mentioned reasons, various solutions are developed for AC regulation and the studies for this area still go on.

In order to regulate the voltage variations of the distribution systems, voltage conditioners [1,2], voltage sag/swell compensators [3,4], voltage sag supporters [5,6], DVRs (dynamic voltage restorers) [7,8], etc., that are FACTS (flexible AC transmission systems) devices, are successfully incorporated to the power systems and efficient results are achieved. By these devices, the provision of the requested distribution network voltages for the buses of the AC loads can be obtained. For this reason, it cannot be possible to regulate individual AC loads voltages by this technique. An additional coupling transformer is required for these VSIs (voltage source inverter) based FACTS devices regulators. A DC-AC converter topology or an AC-DC-AC converter topology may be constructed for the mentioned FACTS devices' VSIs. Batteries or capacitors that are independent external DC storage systems are required for the DC-AC converter-based VSIs. For this reason, VSIs based on DC-AC converters are not capable of accurate compensation of voltage sags or voltage swells. In addition external storage unit capacities restrict the capabilities of the AC-DC-AC converters-based VSIs incorporate AC-DC structure in the main topology. Thus, need for external storage systems is not necessary in AC-DC-AC converters. Nevertheless, increased total loss of the AC-DC-AC converter-based FACTS devices, because of the additional AC-DC unit, brings a disadvantage compared to the DC-AC based FACTS regulators.

In order to avoid using an additional coupling transformer like in the FACTS-based regulators, AC-DC-AC based VSIs may be applied directly for voltage regulation for AC loads [9,10]. Another advantage of the mentioned VSIs is that they can regulate the voltages of each AC load through the distribution voltages, if the distribution voltage is in the determined level or not. Nevertheless, direct AC-AC conversion is not possible in these VSIs. Total AC-AC conversion is done in two stages, AC to DC and then DC to AC conversion. It is clear that this increases the total loss and this causes a disadvantage for using VSIs for voltage regulation.

Apart from the regulation solutions mentioned above, it is evident that direct AC to AC conversion provides superiority regarding less complexity and improved voltage regulation capabilities. Many kinds of AC-AC regulator topologies are proposed by the researchers in the literature. AC-AC PWM-based choppers can provide desirable AC voltage regulation [11]. Because of chopping the input sine wave to regulate the output voltage level, the output voltage includes high-level high-frequency harmonics and it is far from the ideal sine wave. Because of this situation, using additional filtering units such as passive filters or coupling transformers is essential to reduce the harmonics of the regulator output voltage. The researchers study AC-AC regulators based on switch-mode operation such as buck [12-16], boost [17,18], and buck-boost [19,20] type regulators for AC regulation for a long time. As the mentioned AC-AC regulators operate in switch-mode and have an internal filtering structured topology, close to sine-wave output voltages without the need for additional filtering units to eliminate the output voltage harmonics can be provided. Reduced number of elements is required in

these regulator topologies. The in the literature proposed switch-mode AC-AC regulators obtain successful results. However, input AC voltages are assumed as ideal sine waves in these studies and non-sinusoidal input voltage cases are not considered. But, because of distortions in distribution networks, the input supply voltages of the AC loads can have harmonics and can be far from sine wave. Because of this, AC-AC regulators must eliminate the voltage harmonics during the AC regulation process. As the AC loads have to be supplied by as close as possible to ideal sine-wave voltages, where THD is under 5% [21], the harmonic elimination capability of AC-AC regulators becomes an important issue.

A three-phase buck-type active tracking AC-AC voltage regulator is developed in this paper. For the active tracking of the demanded reference output sine-wave phase voltages, an improved control technique is presented for the regulator operation control. The proposals for the regulator topology and the control technique are patented by the co-author of this paper [22]. The proposed regulator topology has a reduced numbers of components, just twelve switches, three capacitors, and three inductors. The buck-type structure of the proposed three-phase regulator allows to obtain voltage amplitudes for each output phase that is lower than the input voltage amplitudes of each input phase in a wide range. The regulator topology has a modular structure for independent control of each output phase. So, the regulator can achieve close to sine-wave output phase voltages to supply a balanced/unbalanced wye-connected three-phase load or independent single-phase loads. The proposed control technique has a new hybrid control structure unlike similar studies in the literature. A closed-loop PID controller is supported by a new feedforward controller in this hybrid control technique. In this way, an enhancement of the active tracking of the reference sine-wave output phase voltages is provided to obtain as close as possible sine-wave output phase voltages, when the input phase voltages are either pure sines or not. The presented three-phase regulator and the control technique are tested with simulation and experimental studies. The results have demonstrated that the proposed switch-mode three-phase buck-type active tracking voltage regulator can provide the desired AC phase voltages including lower than 5% THD harmonics for different operating conditions.

II. THE THREE-PHASE BUCK AC-AC REGULATOR

In this section, the topology of the proposed three-phase AC-AC regulator based on the buck converter, as well as the regulator's operation procedure and the dynamic analysis are described.

A. THE REGULATOR'S TOPOLOGY

Figure 1 shows the main circuit of the proposed three-phase AC-AC regulator based on the buck converter [22].

As seen in Figure 1, the proposed three-phase AC-AC regulator is comprised of three buck converter based sub-circuits that are connected to each other as wye-connection at a common point. This point is the neutral point (N). The second-order subscripts "1,2,3" represent the phase number of the three-phase and this is represented generally in the study as "n" where n=1,2,3. To have a neutral return, the regulator sub-circuits' neutral point N and the three-phase load neutral are linked together. So, modular three independent single-phase or three-phase unbalanced regulator operation can also be achieved by the structure of the proposed regulator topology.

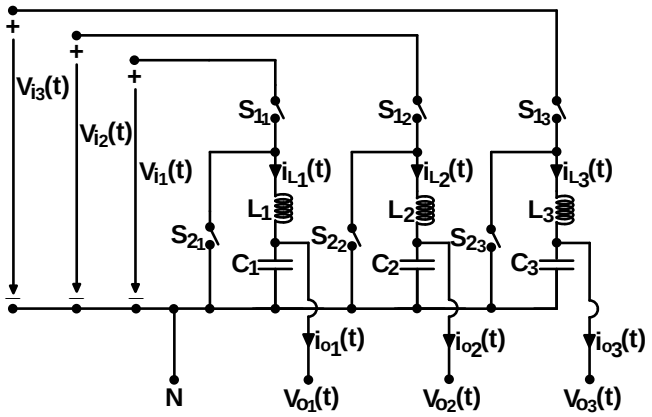

Figure 1. *General topology of the proposed three-phase buck-type AC-AC regulator*

Input AC phase voltages, output AC phase voltages, inductors, and capacitors are represented by V_{in}, V_{on}, L_n, and C_n, respectively in Figure 1. S_{1n} and S_{2n} are the bidirectional active switches. S_{1n} and S_{2n} are realized with IGBTs. So, the proposed regulator circuit, where IGBTs are used, can be given in Figure 2.

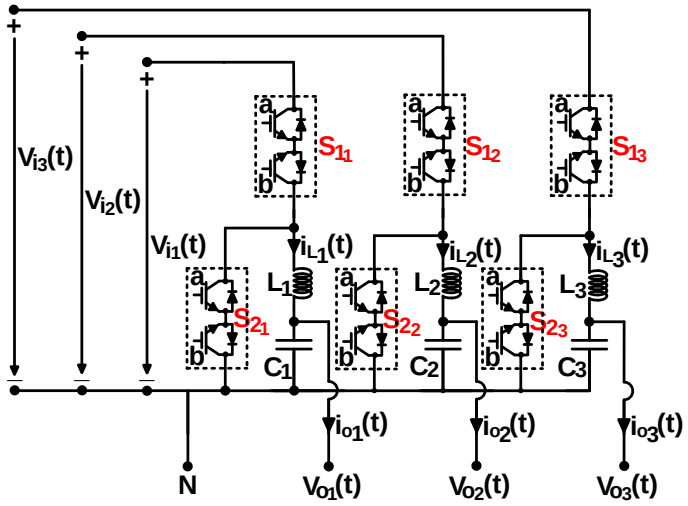

Figure 2. *Proposed three-phase buck-type AC-AC regulator with IGBTs*

B. THE REGULATOR'S OPERATION PROCEDURE

The proposed three-phase AC-AC regulator's operation procedure is based on the well-known traditional buck converter. In the study, each phase sub-circuits is structured identically. The instant input phase voltages $V_{in}(t)$ are bucked at the output and $V_{on}(t)$ phase output voltages are obtained based on the control of PWM duty ratios (d_n) of S_{1n}. In this way, the output phase voltages are produced as AC phase voltages with the same polarity as the input phase voltages, but with lower amplitude values than that of the input phase voltage values. S_{2n} play the roles as the supplementary switches of S_{1n}. While S_{1n} are turned on, S_{2n} are turned off. The inductors, capacitors and output phase loads are supplied by V_{in} in this stage. While S_{1n} are turned off, S_{2n} are turned on. The pre-energized inductors supply the capacitors and output phase the loads in this stage.

The V_{in} input phase voltages' polarities change at each half period, because the input phase voltages V_{in} are alternating voltages. Thus, the on-off states of the sub-active switches of the bidirectional active switches S_{1n} and S_{2n} need to change for each half-period of the input phase voltages depending on the polarities. In Table 1, the details for control of S_{1n} and S_{2n} active switches are shown in detail.

Table 1. *Control signal of IGBTs used in Figure 2 as part of the bidirectional S_{1n} and S_{2n} active switches.*

State	S_{1n}				S_{2n}			
	Positive Half-Wave Stage		Negative Half-Wave Stage		Positive Half-Wave Stage		Negative Half-Wave Stage	
	S_{1an}	S_{1bn}	S_{1an}	S_{1bn}	S_{2an}	S_{2bn}	S_{2an}	S_{2bn}
ON	on	off	off	on	off	on	on	off
OFF	off	off	off	off	off	off	off	off

Figure 3 summarizes the IGBTs' switching pattern in detail.

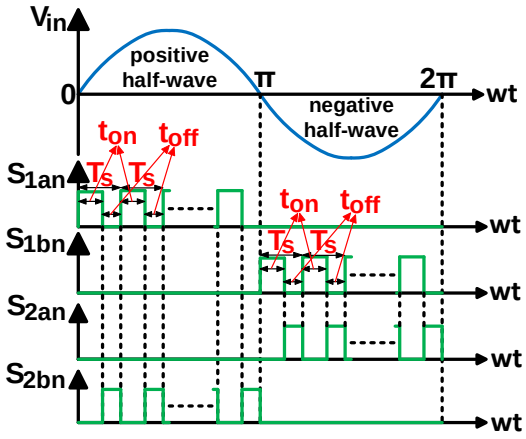

Figure 3. *Switching pattern of the IGBTs*

Figure 4 summarizes the equivalent sub-circuits of the proposed regulator topology for one cycle sine-wave input voltage depending on Figure 2 and the proper control of the active switches as given in Table 1.

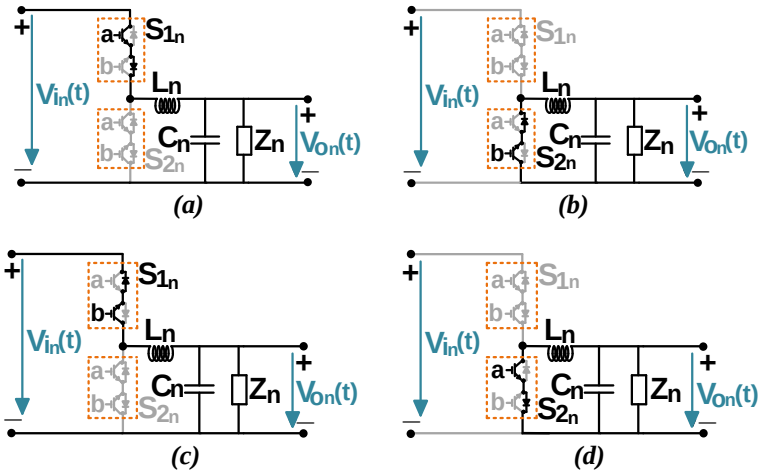

Figure 4. *Equivalent sub-circuits of the proposed buck type regulator* ***(a)*** *Positive half-wave output stage, on mode (S_{1n} is on, S_{2n} is off),* ***(b)*** *Positive half-wave output stage, off mode (S_{1n} is off, S_{2n} is on),* ***(c)*** *Negative half-wave output stage, on mode (S_{1n} is on, S_{2n} is off),* ***(d)*** *Negative half-wave output stage, off mode (S_{1n} is off, S_{2n} is on)*

So, the two main stages given below summarize the proposed regulator's output phase voltage producing operation for one cycle according Figure 3 and Figure 4.

Stage 1 ($0 \leq wt < \pi$): In this stage, the input phase voltage is in positive half-wave periods regarding the defined polarities. While the PWM on-stages of S_{1n} (S_{2n} are off), S_{1an} are turned on, S_{1bn} are turned off

and both S_{2an} and S_{2bn} are turned off. While the PWM off-stages of S_{1n} (S_{2n} are on), both S_{1an} and S_{1bn} are turned off, S_{2an} are turned off, and S_{2bn} are turned on. The positive half sine-wave phase output voltages are generated by the phase input voltages based on the continuous proper control of d_n that are the PWM duty ratios of S_{1n}.

Stage 2 ($\pi \leq wt < 2\pi$): In this stage, the input phase voltage is in negative half-wave periods regarding the defined polarities. While the PWM on-stages of S_{1n} (S_{2n} are off), S_{1bn} are turned on, S_{1an} are turned off and both S_{2an} and S_{2bn} are turned off. While the PWM off-stages of S_{1n} (S_{2n} are on), both S_{1an} and S_{1bn} are turned off, S_{2bn} are turned off, and S_{2an} are turned on. The negative half sine-wave phase output voltages are generated by the phase input voltages based on the continuous proper control of d_n that are the PWM duty ratios of S_{1n}.

C. THE DYNAMIC ANALYSIS

This section gives the detailed dynamic analysis of the proposed three-phase AC-AC regulator based on buck converter. In order to provide precise analysis for real-time applications, parasitic effects of the elements used in the topology are taken into account during the analysis.

The proposed regulator's equivalent circuit for the positive half-wave input stage is given in detail in Figure 5. The same IGBTs used in the study are selected. So the equivalent circuits in Figure 5 are valid for each phase sub-circuits.

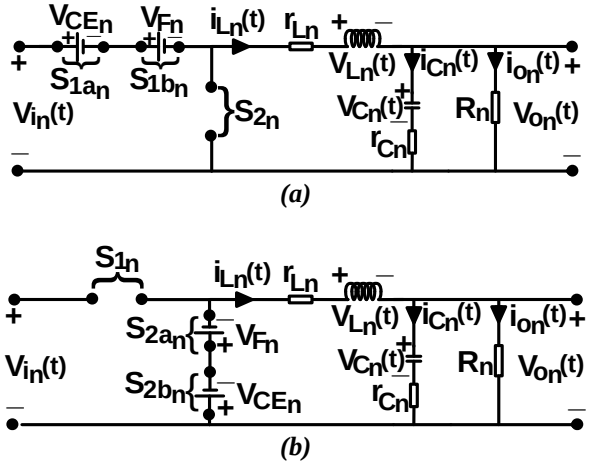

Figure 5. *Positive half-wave stage equivalent circuit of the regulator* ***(a)*** *on-mode – S_{1n} is turned on and S_{2n} is turned off,* ***(b)*** *off-mode – S_{1n} is turned off and S_{2n} is turned on*

In Figure 5, i_{on}, i_{Ln}, i_{Cn}, V_{Ln}, V_{Cn}, V_{Fn}, V_{CEn}, r_{Ln}, r_{Cn}, and R_n represent the output currents, inductor currents, capacitor currents, inductor voltages, capacitor voltages, forward biasing voltages of the IGBTs' anti-parallel diodes, collector-emitter on-voltages of the IGBTs, equivalent series resistances (ESRs) of the inductors, ESRs of the capacitors, and output phase load resistances, respectively.

The regulator's dynamic analysis can be done for the positive half-wave input stage according Figure 5. The dynamic equations of the output voltages and inductor currents can be obtained for the two modes, on-mode and off-mode from Figure 5.

On-mode (S_{1n} are on and S_2 are off): The inductor currents' and the output voltages' state equations can be obtained from Figure 5*a* for on-mode, respectively as follows.

$$\frac{di_{L_n}(t)}{dt} = -\frac{1}{L_n} r_{L_n} i_{L_n}(t) - \frac{1}{L_n} V_{o_n}(t) + \frac{1}{L_n}\left[V_{i_n}(t) - V_{CE_n} - V_{F_n}\right] \quad (1)$$

$$\frac{dV_{o_n}(t)}{dt}=\frac{R_n}{R_n+r_{C_n}}\left[\frac{1}{C_n}-\frac{r_{C_n}r_{L_n}}{L_n}\right]i_{L_n}(t)-\frac{R_n}{R_n+r_{C_n}}\left[\frac{r_{C_n}}{L_n}+\frac{1}{R_nC_n}\right]V_{o_n}(t)+\frac{r_{C_n}R_n}{\left(R_n+r_{C_n}\right)L_n}\left[V_{i_n}(t)-V_{CE_n}-V_{F_n}\right] \quad (2)$$

Off-mode (S_{1n} are off and S_2 are on): The inductor currents' and the output voltages' state equations can be obtained from Figure 5*b* for off-mode, respectively as follow.

$$\frac{di_{L_n}(t)}{dt}=-\frac{1}{L_n}r_{L_n}i_{L_n}(t)-\frac{1}{L_n}V_{o_n}(t)-\frac{1}{L_n}\left[V_{CE_n}+V_{F_n}\right] \quad (3)$$

$$\frac{dV_{o_n}(t)}{dt}=\left(\frac{R_n}{R_n+r_{C_n}}\right)\left[\frac{1}{C_n}-\frac{r_{C_n}r_{L_n}}{L_n}\right]i_{L_n}(t)-\left(\frac{R_n}{R_n+r_{C_n}}\right)\left(\frac{r_{C_n}}{L_n}+\frac{1}{R_nC_n}\right)V_{o_n}(t)-\frac{r_{C_n}R_n}{\left(R_n+r_{C_n}\right)L_n}\left[V_{CE_n}+V_{F_n}\right] \quad (4)$$

Through (1) and (2), the state-space model equations of on-mode can be determined as shown below,

$$\begin{bmatrix}\dot{i}_{L_n}(t)\\ V_{o_n}(t)\end{bmatrix}=\begin{bmatrix}-\frac{r_{L_n}}{L_n} & -\frac{1}{L_n}\\ \frac{R_n}{R_n+r_{C_n}}\left[\frac{1}{C_n}-\frac{r_{C_n}r_{L_n}}{L_n}\right] & -\frac{R_n}{R_n+r_{C_n}}\left[\frac{r_{C_n}}{L_n}+\frac{1}{R_nC_n}\right]\end{bmatrix}\begin{bmatrix}i_{L_n}(t)\\ V_{o_n}(t)\end{bmatrix}+\begin{bmatrix}\frac{1}{L_n} & -\frac{1}{L_n} & -\frac{1}{L_n}\\ \left(\frac{R_n}{R_n+r_{C_n}}\frac{r_{C_n}}{L_n}\right) & -\left(\frac{R_n}{R_n+r_{C_n}}\frac{r_{C_n}}{L_n}\right) & -\left(\frac{R_n}{R_n+r_{C_n}}\frac{r_{C_n}}{L_n}\right)\end{bmatrix}\begin{bmatrix}V_{i_n}(t)\\ V_{CE_n}\\ V_{F_n}\end{bmatrix} \quad (5)$$

Through (3) and (4), the state-space model equations of off-mode can be determined as below,

$$\begin{bmatrix}\dot{i}_{L_n}(t)\\ V_{o_n}(t)\end{bmatrix}=\begin{bmatrix}-\frac{r_{L_n}}{L_n} & -\frac{1}{L_n}\\ \frac{R_n}{R_n+r_{C_n}}\left[\frac{1}{C_n}-\frac{r_{C_n}r_{L_n}}{L_n}\right] & -\frac{R_n}{R_n+r_{C_n}}\left(\frac{r_{C_n}}{L_n}+\frac{1}{R_nC_n}\right)\end{bmatrix}\begin{bmatrix}i_{L_n}(t)\\ V_{o_n}(t)\end{bmatrix}+\begin{bmatrix}0 & -\frac{1}{L_n} & -\frac{1}{L_n}\\ 0 & -\left(\frac{R_n}{R_n+r_{C_n}}\frac{r_{C_n}}{L_n}\right) & -\left(\frac{R_n}{R_n+r_{C_n}}\frac{r_{C_n}}{L_n}\right)\end{bmatrix}\begin{bmatrix}V_{i_n}(t)\\ V_{CE_n}\\ V_{F_n}\end{bmatrix} \quad (6)$$

As mentioned before, the dynamic analysis presented above is derived for the positive half-wave input case. The same state-space equations of (5) and (6) can also be derived when a similar dynamic analysis is performed for the negative half-wave input case. Thus, it is clear that the state-space equations (5) and (6) provide the validity for both negative and positive half-wave input cases. So, the small signal transfer functions between PWM duty ratios and the output phase voltages can be determined using (5) and (6) as

$$G_{buck_n}(s)=\frac{\hat{V}_{o_n}(s)}{d_n(s)}=\frac{g_n s+\left(a_n g_n+c_n f_n\right)}{s^2+\left(a_n+e_n\right)s+\left(a_n e_n-b_n c_n\right)}. \tag{7}$$

The coefficients used in (7) are:

$$a_n=\frac{r_{L_n}}{L_n} \tag{8}$$

$$b_n=-\frac{1}{L_n} \tag{9}$$

$$c_n=\frac{R_n}{R_n+r_{C_n}}\left[\frac{1}{C_n}-\frac{r_{C_n}r_{L_n}}{L_n}\right] \tag{10}$$

$$e_n=\frac{R_n}{R_n+r_{C_n}}\left[\frac{r_{C_n}}{L_n}+\frac{1}{R_n C_n}\right] \tag{11}$$

$$f_n=\frac{\bar{V}_{i_n}}{L_n} \tag{12}$$

$$g_n=\frac{r_{C_n}R_n}{\left(R_n+r_{C_n}\right)L_n}\bar{V}_{i_n} \tag{13}$$

In (12)-(13), $\bar{V}_{i_n}$ define the input phase voltages at the operating point.

III. THE PROPOSED HYBRID CONTROL TECHNIQUE FOR THE REGULATOR'S OPERATION

In this section, the proposed hybrid control technique, which is applied for the control of the proposed AC-AC regulator, is given in detail. Figure 6 shows the general control diagram of the proposed regulator.

As seen in Figure 6, the PLLs provide determine the frequencies and the wave-form of the reference signal of the AC phase voltages and V_{rn} determine the magnitudes of the reference output AC phase voltages. So, the desired sine-wave reference AC output phase voltages can be obtained according to

$$\left.\begin{aligned} V_{ref_1}(wt)&=V_{r_1}\sin w_1 t\\ V_{ref_2}(wt)&=V_{r_2}\sin\left(w_2 t-120^o\right)\\ V_{ref_3}(wt)&=V_{r_3}\sin\left(w_3 t+120^o\right)\end{aligned}\right\}. \tag{14}$$

As demonstrated in Figure 6, the proposed hybrid controller is constructed with two main units. One of these units is the traditional closed-loop PID controller. The PID controller eliminates of the error between the real output voltage and the reference and satisfies the desired response performance in the design. The hybrid controller's other unit is the feedforward controller. It is developed in this study and called "control law (CL)" as seen in Figure 6. Open-loop based CL provides a PWM duty ratio regarding the topology parameters as given below.

$$d_{CL_n}(wt) = \sqrt{\frac{2L_n\left|V_{r_n}\sin w_n t\right|\left(\left|V_{r_n}\sin w_n t\right| + V_{CE_n} + V_{F_n}\right)}{\left|V_{i_n}(wt)\right|\left(\left|V_{i_n}(wt)\right| - \left|V_{r_n}\sin w_n t\right| - V_{CE_n} - V_F\right)T_{S_n}R_n}} \tag{15}$$

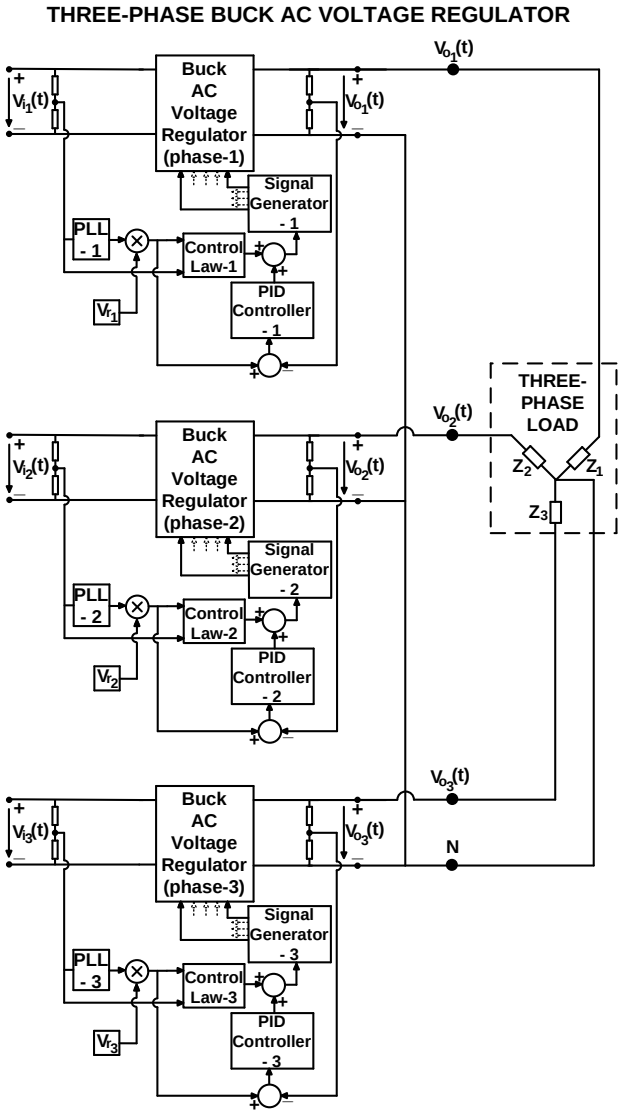

Figure 6. *General control diagram of the proposed regulator*

T_S represents the PWM switching period in (15). It is not possible to achieve the reference output voltage only by the PWM duty ratio of the CL in (15). But the duty ratio produced by the CL provides a close value to the real duty ratio. (16) shows that the CL has a static structure that can provide a duty ratio and the duty ratio can be obtained in a fast manner. Thus, the requested operating duty ratio works with an enhanced response performance by supporting the PID controller with the CL. In this way, close to ideal sine-waves with low THD can be achieved by the proposed hybrid control as the proposed hybrid control technique provides an active tracking of the reference output voltage in an

efficient and accurate manner. Thus, the CL and the PID controller generate the requested operating PWM duty ratio together as

$$d_n(wt) = d_{PID_n}(wt) + d_{CL_n}(wt) \tag{16}$$

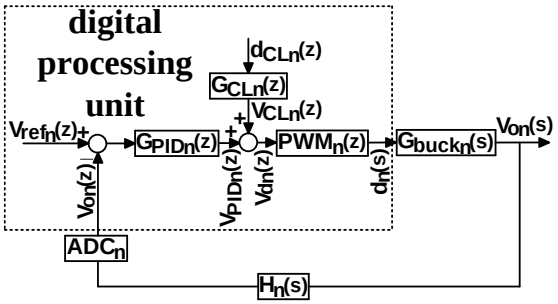

Figure 7. *Discrete-time control block diagram based on the proposed hybrid control technique for the buck-type 3-phase regulator*

Discrete-time control is chosen for the control of the regulator operation in this paper. Thereby, in Figure 7, the control block diagram of the regulator based on the proposed hybrid control technique can be depicted.

The equations given below which define the relations between the transfer functions and the control signals of the discrete-time control block diagram can be obtained from Figure 7.

$$G_{CL_n}(z) = \frac{1}{PWM_n(z)} \tag{17}$$

$$V_{d_n}(z) = V_{CL_n}(z) + V_{PID_n}(z) \tag{18}$$

$$d_n(z) = V_{d_n}(z).PWM_n(z) \tag{19}$$

The determined PID controller's transfer function can be expressed in this paper as follows

$$G_{PID_n}(z) = K_{P_n} + K_{I_n}\frac{z}{z-1} + K_{D_n}\frac{z-1}{z} \tag{20}$$

IV. THE SIMULATION AND EXPERIMENTAL RESULTS

The design steps of the proposed regulator are determined and the regulator study results for both the simulation and the experimental tests are given in this section.

A. THE DESIGN CRITERIA FOR THE REGULATOR STUDY

An experimental laboratory set-up of the proposed regulator is built to verify the real-time experimental performance of the proposed regulator. The set-up is designed for 2.2 kW output power, 0-300 Vp input phase voltages (50 Hz), and 0-200 Vp output phase voltages. IXGH20N60BU1 type n-channel high-speed IGBTs (V_{CES}=600 V, V_{CE}=1.7 V, V_F=1.6 V, I_C=40 A) are chosen as the active switches in the set-up topology. Table 2 demonstrates the chosen values of the capacitors, the inductors, and the switching frequencies for the regulator circuit's phase sub-units.

Table 2. *The selected values of the switching frequencies, inductors and capacitors.*

Switching Frequencies f_{sn} *(kHz)*	**Capacitors**		**Inductors**	
	C_n *(μF)*	**r_{Cn}** *($m\Omega$)*	**L_n** *(μH)*	**r_{Ln}** *($m\Omega$)*
50	15	200	50	150

In Table 3, the determined operating point parameters which are used in the discrete time PID controllers design for the phase sub-units are given.

Table 3. *The considered operating point parameters of the regulator operation*.

$\bar{V}_{i_n}$ *(V)*	$\bar{D}_n$	$\bar{V}_{o_n}$ *(V)*	**R_n** *(Ω)*
150	0.5	75	30

The parameters of the PID controller used in (21) are obtained through the optimum design and performance analysis in MATLAB-Sisotool as can be seen below

$$K_{P_n} = -0.045, \quad K_{I_n} = 0.1064, \quad K_{D_n} = 0.0073 \tag{21}$$

B. THE RESULTS OF THE SIMULATION STUDIES

Simulation tests with the proposed hybrid control approach are used to validate the theoretical proposals of the study.

Table 4 gives the applied three different simulation test cases in MATLAB Simulink to the regulator system. Figures 8-10 demonstrate the wave form test results for the simulation studies. Table 5 also gives the numerical results of the simulation tests for the output in detailed. THD_{In} and THD_{Vn} in Table 5 are the THD values for currents and voltages, respectively.

Table 4. *Test cases of the simulation studies.*

Test Case No	**V_{in}** *(V)*			**Output Load Z_n**			**Desired output fundamental sine-wave voltage V_{on}** *(V)*		
	V_{i1}	**V_{i2}**	**V_{i3}**	**Z_1**	**Z_2**	**Z_3**	**V_{o1}**	**V_{o2}**	**V_{o3}**
1	200V sine (f=50Hz)	240V sine (f=50Hz)	180V sine (f=50Hz)	Resistive R_1=20Ω	Resistive R_2=20Ω	Resistive R_3=20Ω	150	150	150
2	150V sine (f=50Hz)	175V sine + LOH (f=50Hz)	220V sine + HOH (f=50Hz)	Inductive R_1=6Ω, L_1=4.7mH	Inductive R_2=6Ω, L_2=4.7mH	Inductive R_3=6Ω, L_3=4.7mH	100	100	100
3	160V sine + HOH (f=50Hz)	120V sine + fluct. (f=50Hz)	100V sine + LOH (f=50Hz)	Resistive R_1=10Ω	Inductive R_2=8Ω, L_2=6.8mH	Capacitive R_3=5Ω, C_3=0.5mF	50	70	85

fluct.: fluctuations, HOH: high order harmonics, LOH: low order harmonics

The results given in Figures 8-10 and Table 5 show that the proposed three-phase AC-AC regulator based on the buck converter can produce the desired reference AC phase sine-wave voltages with under 5% THD values, where the three-phase output is unbalanced and the input AC phase voltages

include harmonics components. It is clear from the achieved results that the proposed three-phase AC-AC regulator based on the buck converter is capable of operating in independent single-phase loading in modular mode. As a result, the accurate and efficient active tracking of the reference phase output voltages of the proposed hybrid control technique is revealed by the achieved numerical results in Table 5 and wave form results in Figures 8-10.

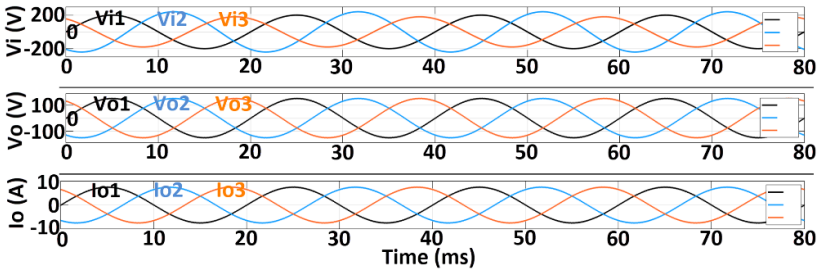

Figure 8. *Simulation results for test case-1*

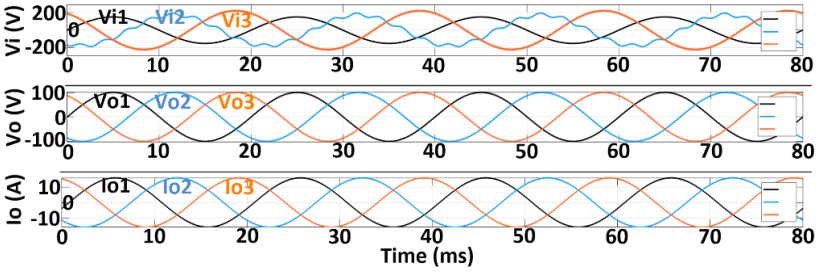

Figure 9. *Simulation results for test case-2*

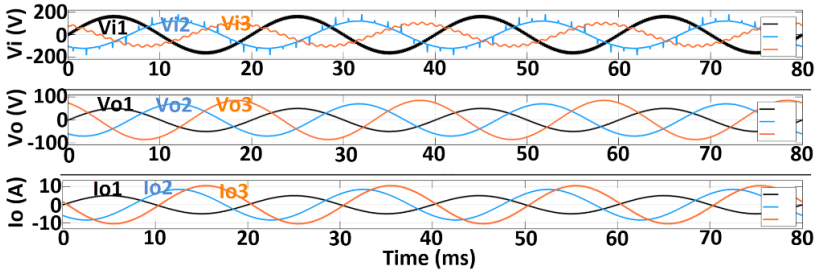

Figure 10. *Simulation results for test case-3*

Table 5. *The achieved numerical simulation results of the test cases.*

Test Case No	Obtained Fundamental V_{on} *(V)*			THD_{Vn} *(%)*			THD_{In} *(%)*		
	V_{o1}	V_{o2}	V_{o3}	THD_{V1}	THD_{V2}	THD_{V3}	THD_{I1}	THD_{I2}	THD_{I3}
1	150.2	150.2	150.2	2.06	2.06	2.06	2.06	2.06	2.06
2	100.3	100.3	100.3	2.11	2.11	2.11	2.03	2.03	2.03
3	50.1	69.9	84.7	1.93	1.87	2.01	1.93	1.79	2.16

C. THE RESULTS OF THE EXPERIMENTAL STUDIES

Experimental tests with the proposed hybrid control approach are used to validate the real-time practical application of the study. Figure 11 depicts the experimental set-up that is designed for the regulator system.

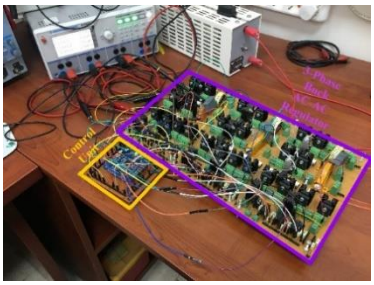

Figure 11. *The designed experimental set-up of the regulator system*

Table 6 shows the applied three different experimental test cases on the laboratory set-up to the regulator system. Figures 12-14 demonstrate the wave form test results for the experimental studies. Table 7 also gives the numerical results of experimental tests for the output in detail.

Table 6. *Test cases of the experimental studies.*

Test Case No	**V_{in}** *(V)*			**Output Load Z_n**			**Desired output fundamental sine-wave voltage V_{on}** *(V)*		
	V_{i1}	**V_{i2}**	**V_{i3}**	**Z_1**	**Z_2**	**Z_3**	**V_{o1}**	**V_{o2}**	**V_{o3}**
1	150V sine (f=50Hz)	200V sine (f=50Hz)	180V sine (f=50Hz)	Resistive R_1=30Ω	Resistive R_2=30Ω	Resistive R_3=30Ω	120	120	120
2	160V sine (f=50Hz)	120V sine (f=50Hz)	100V sine (f=50Hz)	Inductive R_1=10Ω, L_1=10mH	Inductive R_2=10Ω, L_2=10mH	Inductive R_3=10Ω, L_3=10mH	80	80	80
3	175V sine (f=50Hz)	175V sine (f=50Hz)	175V sine (f=50Hz)	Resistive R_1=20Ω	Inductive R_2=7Ω, L_2=2.2mH	Capacitive R_3=20Ω, C_3=0.33mF	100	50	65
fluct.: fluctuations, HOH: high order harmonics, LOH: low order harmonics									

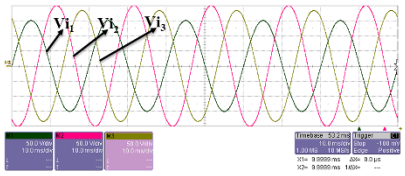

(a)

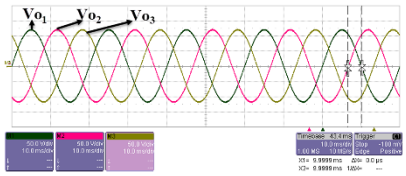

(b)

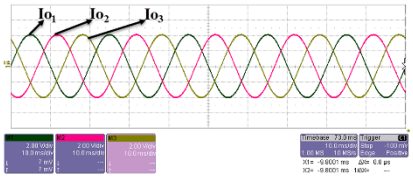

(c)

Figure 12. *Experimental results for the test case-1 (V/div=A/div for I_{On})* ***(a-c)***

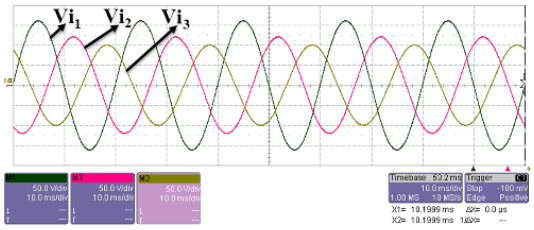

(a)

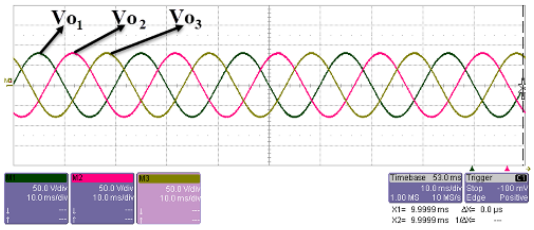

(b)

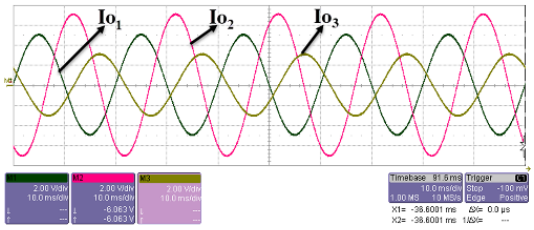

(c)

Figure 13. *Experimental results for the test case-2 (V/div=A/div for I_{On})* ***(a-c)***

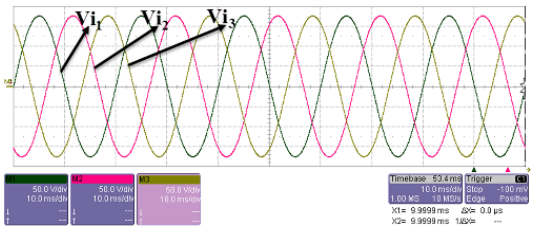

(a)

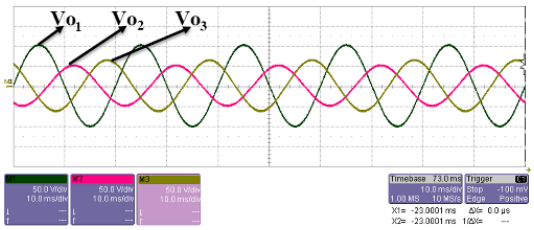

(b)

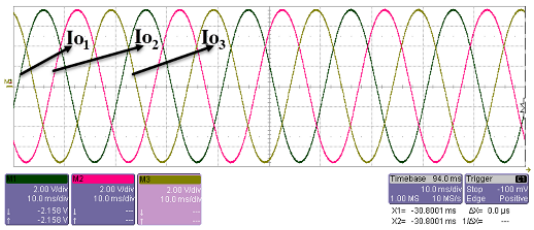

(c)

Figure 14. *Experimental results for the test case-3 (V/div=A/div for I_{On})* ***(a-c)***

Table 7. *The achieved numerical experimental results of the test cases.*

Test Case No	Obtained Fundamental V_{on} *(V)*			THD_{Vn} *(%)*			THD_{In} *(%)*		
	V_{o1}	V_{o2}	V_{o3}	THD_{V1}	THD_{V2}	THD_{V3}	THD_{I1}	THD_{I2}	THD_{I3}
1	120.4	120.4	120.4	1.95	1.99	1.98	1.90	1.96	1.94
2	80.3	80.3	80.1	1.75	1.82	1.86	1.61	1.70	1.73
3	100.2	49.9	65.1	2.19	2.10	2.02	2.14	1.91	2.19

The results given in Figures 12-14 and Table 7 show that the proposed three-phase AC-AC regulator based on buck converter can produce the desired reference AC phase sine-wave voltages experimentally with under 5% THD values, where the three-phase output is unbalanced. In this study, the experimental voltage and current THD values are measured and transferred to MATLAB. The related transferred waveforms are analyzed in MATLAB and voltage/current THD values are obtained by analyzing these waveforms. It is also clear from the achieved results that the proposed three-phase AC-AC regulator based on buck converter is capable of operating in independent single-phase loading in modular mode. As a result, the accurate and efficient active tracking of the reference phase output voltages of the proposed hybrid control technique is revealed experimentally through the achieved numerical results in Table 7 and wave form results in Figures 12-14.

A comparative test study is performed to demonstrate the efficient active reference phase output voltages tracking of the proposed hybrid control. The proposed hybrid control technique and the standalone PID control are applied to the proposed regulator separately for the experimental test case-3 in this comparative test application. Figure 15 depicts the provided phase-2 output voltage waveforms for the mentioned two separate applications together. Table 8 also show the comparative numerical output THD results of these comparative applications.

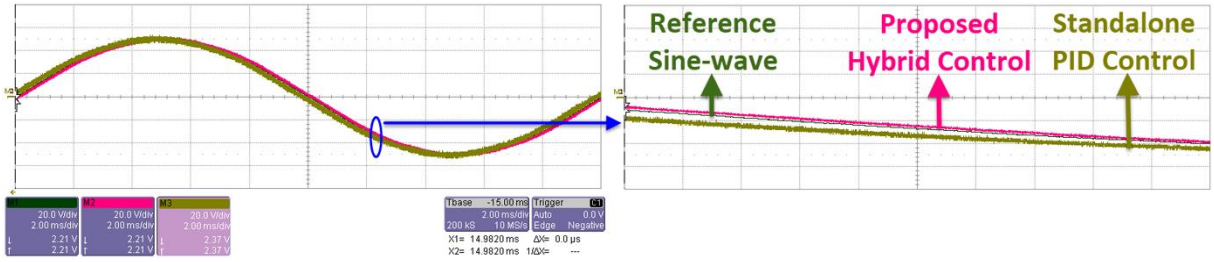

Figure 15. *Comparative output phase-2 voltage V_{o2} wave forms of the proposed hybrid control and the standalone PID control for the test case-3 (20V/div, 2ms/div)*

Table 8. *Comparative THD results of the proposed hybrid control and the standalone traditional PID control for the experimental test cases.*

Test Case No	THD results of the proposed hybrid control method *(%)*						THD results of the traditional standalone PID control *(%)*					
	THD_{Vn}			THD_{In}			THD_{Vn}			THD_{In}		
	THD_{V1}	THD_{V2}	THD_{V3}	THD_{I1}	THD_{I2}	THD_{I3}	THD_{V1}	THD_{V2}	THD_{V3}	THD_{I1}	THD_{I2}	THD_{I3}
1	1.95	1.99	1.98	1.90	1.96	1.94	2.09	2.10	2.08	1.99	2.05	2.06
2	1.75	1.82	1.86	1.61	1.70	1.73	1.83	1.90	1.98	1.74	1.77	1.87
3	2.19	2.10	2.02	2.14	1.91	2.19	2.28	2.21	2.09	2.27	2.04	2.29

Figure 15 proves that better active tracking of the reference phase output sine-wave voltages can be provided through the proposed hybrid control technique than the standalone traditional PID control. As a result, enhancing the active tracking capability of the developed CL by supporting the PID controller is proved. The efficiency of the proposed hybrid control technique can also be proved by the obtained output THD results as seen in Table 8. The less than 5% THD results in Table 8 show how the proposed hybrid control technique provides high quality close to sine-wave phase output voltages.

The efficiency of the proposed three-phase regulator based on buck converter is analyzed for various output power rates considering the regulator power rate limited in the design. Figure 16 demonstrates the efficiency of the regulator and proves that good enough efficiency can be provided by the proposed regulator.

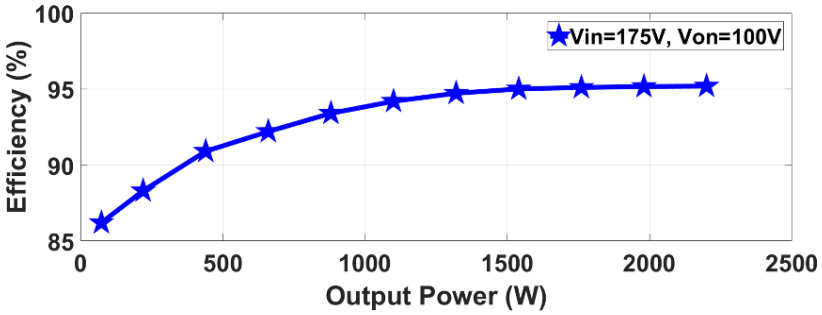

Figure 16. *Efficiency curve of the regulator for different output power rates*

V. CONCLUSION

In this study, a buck converter-based switch-mode active tracking AC-AC three-phase voltage regulator is proposed. The proposed regulator has less complexity and a high-efficiency topology including a moderate number of passive and active components. The developed hybrid control technique for the regulator control is based on supporting the closed-loop PID controller with the novel designed feedforward controller and provides efficient active tracking of the reference output phase voltages according to similar studies in the literature that use only traditional closed-loop controllers. The proposed hybrid control technique augments the achievement of the output phase voltages as close as to the sine-wave reference output phase voltages, although the input AC phase voltages may have high order harmonics. The proposed regulator has also the ability to operate for balanced/unbalanced wye-connected three-phase loads or independent single-phase loads. The achieved results of simulation and experimental test studies verify the ability, accuracy, and efficiency of the proposed switch-mode three-phase buck-type active tracking voltage regulator and can provide the desired output phase voltages in high quality with under 5% THD levels for various input/output operation conditions.

ACKNOWLEDGEMENTS: The topology and control theory of the proposed AC regulator in the study are patented by the co-author in Austrian Patent Office as “Aktive Netzfilter” (patent no: AT 505460 B1, filed 10.07.2007, applied 15.06.2012).

VI. REFERENCES

[1] J. You, D. M. Vilathgamuwa, N. Ghasemi, and B. Fu, “Virtual resistor-based integrated DC bus voltage conditioner for stability improvement of cascaded power converters,” *IEEE Access*, vol. 7, pp. 95959–95969, 2019.

[2] J. Kaniewski, P. Szczesniak, M. Jarnut, and Z. Fedyczak, “Voltage conditioner and power flow controller based on bipolar matrix-reactance choppers,” *Int. J. Elect. Power Energy Syst.*, vol. 94, pp. 256–266, 2018.

[3] J. Kaniewski, “Three-phase AC/AC converter for voltage sag/swell compensator and phase shifter based on Cuk B2 matrix-reactance chopper,” *Elect. Power Syst. Res.*, vol. 125, pp. 203–210, 2015.

[4] J. Kaniewski, “Three-Phase voltage sag/swell compensator with phase shifter function based on bipolar matrix-reactance chopper,” *Int. Symp. Power Electron. Elect. Dri. Automat. Motion (SPEEDAM)*, 2014, pp. 63–642.

[5] S. Subramanian and M. K. Mishra, “Interphase AC-AC topology for voltage sag supporter,” *IEEE Trans. Power Electron.*, vol. 25, no. 2, pp. 514–518, 2010.

[6] D. M. Lee, T. G. Habetler, R. G. Harley, T. L. Keister, and J. R. Rostron, “A voltage sag supporter utilizing a PWM-switched autotransformer,” *IEEE Trans. Power Electron.*, vol. 22, no. 2, pp. 626–635, 2007.

[7] E. M. Molla and C. C. Kuo, “Voltage quality enhancement of grid-integrated PV system using battery-based dynamic voltage restorer,” *Energies*, vol. 13, no. 21, article number: 5742, 2020.

[8] C. I. Chen, Y. C. Chen, C. H. Chen, and Y. R. Chang, “Voltage regulation using recurrent wavelet fuzzy neural network-based dynamic voltage restorer,” *Energies*, vol. 13, no. 23, article number: 6242, 2020.

[9] P. L. S. Rodrigues, C. B. Jacobina, and N. B. De Freitas, “Single-phase universal active power filter based on ac-dc-ac converter with eight controlled switches,” *IET Power Electron.*, vol. 12, no. 5, pp. 1131–1140, 2019.

[10] N. B. De Freitas, C. B. Jacobina, B. S. Gehrke, and M. F. Cunha, “Transformer-based single-phase AC-DC-AC topology for grid issues mitigation,” *IEEE Trans. Ind. Appl.*, vol. 55, no. 4, pp. 4001–4011, 2019.

[11] Y. B. Wang, G. W. Cai, C. Liu, B. D. Zhu, D. B. Guo, and H. W. Zhang, “Three-phase flexible transformer based on bipolar direct AC/AC chopper and its control strategy,” *IEEE Access*, vol. 8, pp. 173336–173344, 2020.

[12] I. Rankis, M. Prieditis, and G. Stana, “Investigation of direct AC-AC buck converter with series injection transformer,” *IEEE 59th Int. Sci. Conf. Power Elect. Eng. Riga Tech. Uni. (RTUCON)*, 2018.

[13] P. S. Huynh, D. Vincent, N. A. Azeez, L. Patnaik, and S. S. Williamson, “Performance analysis of a single-stage high-frequency AC-AC buck converter for a series-series compensated inductive power transfer system,” *IEEE Transp. Electrif. Conf. Expo (ITEC)*, 2018, pp. 347–352.

[14] J. G. Wang and R. McMahon, “Highly reliable and efficient voltage optimizer based on direct PWM AC-AC buck converter,” *IEEE Trans. Energy Convers.*, vol. 35, no. 4, pp. 1897–1906, 2020.

[15] J. G. Wang and R. McMahon, “Reliable control of direct PWM AC-AC buck converter with short circuit protection,” *IEEE 28th Int. Symp. Ind. Electron. (ISIE)*, 2019, pp. 950–954.

[16] U. A. Khan, A. A. Khan, H. Cha, H. G. Kim, J. Kim, and J. W. Baek, “Dual-buck AC-AC converter with inverting and non-inverting operations,” *IEEE Trans. Power Electron.*, vol. 33, no. 11, pp. 9432–9443, 2018.

[17] O. Ursaru, M. Lucanu, C. Aghion, and N. Lucanu, “Single-phase direct boost AC-AC converter,” *Adv. Elect. Comp. Eng.*, vol. 17, no. 4, pp. 43–48, 2017.

[18] T. Mishima, S. Sakamoto, and C. Ide, “ZVS phase-shift PWM-controlled single-stage boost full-bridge AC-AC converter for high-frequency induction heating applications,” *IEEE Trans. Ind. Electron.*, vol. 64, no. 3, pp. 2054–2061, 2017.

[19] A. A. Khan, H. Cha, and H. F. Ahmed, “An improved single-phase direct PWM inverting buck-boost AC-AC converter,” *IEEE Trans. Ind. Electron.*, vol. 63, no. 9, pp. 5384–5393, 2016.

[20] L. Z. He and X. Y. Xu, “Novel high-efficiency frequency-variable buck-boost AC-AC converter with safe-commutation and continuous current,” *IEEE Trans. Power Electron.*, vol. 35, no. 12, pp. 13225–13238, 2020.

[21] F. Yalcin, U. Arifoglu, I. Yazici, and K. Erin, “Robust single-phase inverter based on the buck-boost converter through an efficient hybrid control,” IET Power Electron., vol. 13, no. 1, pp. 50–59, 2020.

[22] F. Himmelstoss, “Aktive Netzfilter,” Austrian Patent AT 505460 B1, 2012.